

VENOM: Text-driven Unrestricted Adversarial Example Generation with Diffusion Models

Hui Kuurila-Zhang, Haoyu chen, Guoying Zhao*

University of Oulu, CMVS

{hui.zhang, chen.haoyu, guoying.zhao}@oulu.fi



Figure 1. Samples of Natural Adversarial Examples (NAEs) generated by VENOM, conditioned on input text prompts and a designated target label. VENOM achieves nearly a 100% white-box attack success rate in generating NAEs while preserving high image fidelity.

Abstract

Adversarial attacks have proven effective in deceiving machine learning models by subtly altering input images, motivating extensive research in recent years. Traditional methods constrain perturbations within l_p -norm bounds, but advancements in Unrestricted Adversarial Examples (UAEs) allow for more complex, generative-model-based manipulations. Diffusion models now lead UAE generation due to superior stability and image quality over GANs. However, existing diffusion-based UAE methods are limited to using reference images and face challenges in generating Natural Adversarial Examples (NAEs) directly from random noise, often producing uncontrolled or distorted outputs.

In this work, we introduce **VENOM**, the first text-driven framework for high-quality unrestricted adversarial examples generation through diffusion models. VENOM unifies image content generation and adversarial synthesis into a single reverse diffusion process, enabling high-fidelity adversarial examples without sacrificing attack success rate (ASR). To stabilize

this process, we incorporate an adaptive adversarial guidance strategy with momentum, ensuring that the generated adversarial examples x^* align with the distribution $p(x)$ of natural images. Extensive experiments demonstrate that VENOM achieves superior ASR and image quality compared to prior methods, marking a significant advancement in adversarial example generation and providing insights into model vulnerabilities for improved defense development.

1. Introduction

The increasing sophistication of deep learning models has brought about a parallel rise in the need to understand their vulnerabilities, especially through adversarial attacks, where intentionally perturbed inputs, known as adversarial examples [31], are crafted to deceive the victim models with high confidence. These adversarial examples pose a significant threat to the robustness and reliability of deep learning systems. Traditional adversarial attack methods [2, 6, 14, 22] generate adversarial examples by perturbing clean inputs within a restricted l_p -norm ball of magnitude ϵ , aiming to de-

*Corresponding author. Email: guoying.zhao@oulu.fi

ceive the victim models while maintaining the imperceptibility. However, more recent research has introduced Unrestricted Adversarial Examples (UAEs) [30], which are generated without constraints on perturbation magnitude. UAEs can be synthesized directly from random noise using generative models, allowing for more complex transformations beyond pixel-level perturbations. UAEs have demonstrated enhanced attack success rates [3, 7], especially against robust defense methods, compared to traditional, perturbation-based adversarial examples. Initially, Generative Adversarial Networks (GANs) were widely used for generating UAEs [23, 30, 36], but recent diffusion models have outperformed GANs in image quality due to their more stable training process. Diffusion models, by refining the process of image generation, have become the preferred choice for synthesizing UAEs in recent works [3, 4, 7, 21], all of which demonstrated superior performance over GAN-based methods. Importantly, these diffusion-based methods do not require re-training diffusion models for adversarial purposes; rather, they perturb the reverse diffusion process of pre-trained diffusion models to generate UAEs. However, because pre-trained diffusion models are optimized for generating natural images, adversarial guidance during the reverse sampling process can destabilize the generation, resulting in corrupted or unnatural images that may fall outside the distribution of realistic images.

In practice, injecting adversarial guidance into the reverse diffusion process without precise control has led existing diffusion-based UAE generation methods [3, 4, 7, 21] to produce inconsistent results. For instance, [21] often generates adversarial examples that are perceptually invalid, while [7] produces overly perturbed images due to uncontrolled adversarial gradients, [4] suffers from under- or over-perturbed adversarial outputs. While [3] demonstrates stability in generating UAEs from reference images, it is unable to produce Natural Adversarial Examples (NAEs)—a subset of UAEs generated directly from random noise. Hereafter, we use UAE to refer to both UAE and NAE, reserving NAE specifically when emphasizing generation from random noise. Figure 3 illustrates how our proposed method surpasses existing NAE generation approaches [4, 7, 21] in terms of image quality and consistency. The limitations of these prior methods highlight the necessity for a stable, controlled mechanism to generate high-quality UAEs and NAEs that preserve adversarial effectiveness without sacrificing visual realism. To address these challenges, we propose VENOM, a novel framework for stable and high-quality UAE and NAE generation. VENOM introduces an adaptive control strategy to control the injection of gradient-based adversarial guidance, minimizing the risk of image cor-

ruption while maintaining fidelity to the natural image distribution. Additionally, we incorporate a momentum-based technique into the adversarial gradient to enhance transferability and attack strength. Leveraging the Stable Diffusion model [27], along with our adaptive control and momentum modules, VENOM enables text-driven, UAE generation. As the first framework to support fully text-driven UAE generation, VENOM allows users to specify both the visual content and target class of the generated adversarial examples, providing flexibility in crafting adversarial images entirely based on user-defined prompts (see Figure 1).

VENOM achieves near 100% attack success rate (ASR) on white-box models and maintains strong ASR against defense methods while preserving high image fidelity. The framework offers further versatility by supporting both UAE and NAE modes: adversarial examples generated from random noise are classified as NAEs, while those created by perturbing reference images are designated as UAEs.

Our work makes the following key contributions:

- We present VENOM, the first framework, to our knowledge, for text-driven UAEs generation, enabling customized image content and adversarial attack generation purely through text prompts.
- VENOM introduces the first fully-integrated pipeline that combines image content generation and adversarial attack synthesis in a unified reverse diffusion process.
- We propose an adaptive control strategy that precisely modulates adversarial guidance to ensure high image quality with minimal artifacts or distortions. Additionally, we incorporate a gradient-based adversarial guidance mechanism with momentum, compensating for any potential reduction in attack strength from the adaptive control strategy. This approach enables our framework to achieve a balance between image fidelity and adversarial robustness.
- Our framework offers high adaptability, supporting both UAE and NAE modes: generating images from random noise in NAE mode and perturbing reference images in UAE mode.

By addressing the limitations of existing diffusion-based UAE generation methods, VENOM not only advances the state of the art in adversarial example generation but also provides a robust and flexible tool for studying model vulnerabilities. Our approach holds promise for both advancing adversarial robustness research and developing new insights into the potential weaknesses of deep learning systems.

2. Related Work

2.1. Adversarial Examples

The concept of Adversarial Examples (AEs), first introduced by [31], denotes maliciously crafted data generated by applying a small perturbation, δ , to clean data x . This alteration yields a perturbed instance x^* , designed to mislead the victim models into incorrect predictions. Formally, an adversarial example is defined as:

$$x^* = x + \delta \quad \text{s.t.} \quad f(x^*) \neq y \quad \text{and} \quad \|\delta\|_p < \epsilon \quad (1)$$

where f denotes the victim model, y represents the true label, and ϵ bounds the perturbation’s magnitude within an l_p norm to ensure perceptual similarity to x . A variety of algorithms—such as FGSM [14], PGD [22], CW [2], and AutoAttack [6]—have been developed to construct AEs under this constraint.

2.2. Unrestricted Adversarial Examples

Unrestricted Adversarial Examples (UAEs), as the name suggests, extend beyond traditional ϵ -bounded perturbations by allowing adversarial examples without the constraint of small, imperceptible changes. UAEs are defined within the set \mathcal{A} :

$$\mathcal{A} \triangleq \{x \in \mathcal{O} \mid o(x) \neq f(x)\} \quad (2)$$

where \mathcal{O} denotes the set of images perceived as natural and realistic by humans, $o(x)$ represents human evaluation of the image x , and $f(x)$ is the prediction from the victim model. This broader definition permits UAEs to involve transformations such as rotations [1], texture alterations [12, 20], or entirely synthesized images [30]. Generative Adversarial Networks (GANs) have been commonly employed to synthesize UAEs from scratch [23, 30, 36, 38]. However, recent diffusion model-based methods for generating UAEs [3, 4, 7, 21] have highlighted limitations of GAN-based attacks, which suffer from poor image quality and low attack success rates (ASR), especially on large-scale datasets like ImageNet [8]. Specifically, [21] synthesizes UAEs by perturbing text embeddings within Stable Diffusion models, resulting in less distortion. [3] optimizes latent representations by maximizing the likelihood of misclassification. [4] incorporates PGD attack into the reverse diffusion process, while [7] proposes adversarial sampling during the reverse diffusion phase.

2.3. Natural Adversarial Examples

Natural Adversarial Examples (NAEs) are adversarial instances arising from naturally occurring variations in data, as opposed to artificial perturbations, and are defined in Eq. (2). Originally introduced by [16], NAEs represent real-world, out-of-distribution examples that

challenge deep learning models due to distributional shifts [24, 33], such as variations in lighting, viewpoint, or environmental conditions.

We consider NAEs to be a subset of UAEs, as UAEs encompass both naturally occurring adversarial instances and artificially perturbed cases. In some studies, the terms NAEs and UAEs are used interchangeably [4, 21], though NAEs strictly represent a narrower subset of UAEs. In our work, we designate UAEs generated from random noise as NAEs, while UAEs generated by perturbing existing images are simply referred to as UAEs.

3. Method

As discussed in Section 2, previous adversarial attack methods based on diffusion models [3, 4, 7, 21] face a trade-off between the Attack Success Rate (ASR), and image quality. To address this limitation and achieve both high ASR and high image quality, we propose a novel framework designed to stabilize adversarial guidance during the reverse diffusion process by using an adaptive control strategy and momentum, which we term VENOM. The adaptive control strategy and momentum are designed to guide the stable reverse diffusion process to generate adversarial examples, denoted as x^* , from the same distribution $p(x)$ as natural images, ensuring that x^* functions as both a natural and adversarial image simultaneously.

Figure 2 depicts the pipeline for generating adversarial examples from either random noise or reference images using the VENOM algorithm. VENOM offers high flexibility, allowing the generation of adversarial examples based solely on text prompts, with both the target label and reference image being optional. The pipeline is composed of three key modules: the standard reverse diffusion process of the stable diffusion model, adversarial guidance with momentum, and an adaptive control strategy for integrating the adversarial guidance. The following subsections provide a detailed explanation of each module.

3.1. Stable Diffusion

Stable Diffusion [27] is a latent text-to-image diffusion model that incrementally refines random noise into high-quality images guided by text prompts. The approach is rooted in the Denoising Diffusion Probabilistic Model (DDPM) [19], consisting of a forward diffusion phase, where noise is successively added to a clean input z_0 over T discrete time steps, and a reverse phase, aiming to reconstruct the input from a noisy latent z_T .

$$q(z_t|z_{t-1}) = \mathcal{N}(z_t; \sqrt{1 - \beta_t(z_{t-1})}, \beta_t \mathbf{I}), \quad (3)$$

Eq. (3) describes the forward diffusion process, where $\beta_t \in (0, 1)$ is a variance scheduler. z_T is equivalent to

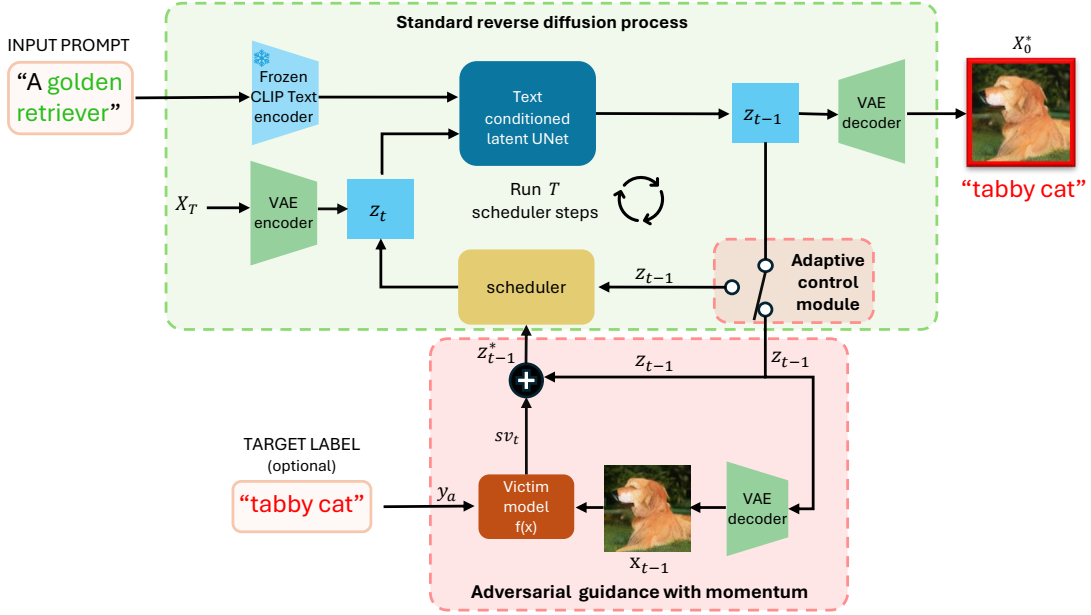


Figure 2. The overview of VENOM algorithm for generating NAEs (no reference images) and UAEs (with reference images). In NAE model, the input X_T is sampled from the standard Gaussian distribution $\mathcal{N}(0, 1)$. In UAE mode, the input X_T is derived by applying the DDIM inversion (Eq. (7)) to the reference image X_0 . If the target label is unavailable, the class with the second-highest likelihood, excluding the ground truth, is assigned as the target label.

an isotropic Gaussian distribution when $T \rightarrow \infty$. By leveraging the properties of Gaussian distributions, the noisy latent at any time step t can be sampled directly from z_0 as shown in Eq. (4), where $\bar{\alpha}_t = \prod_{s=1}^t (1 - \beta_s)$.

$$q(z_t|z_0) = \mathcal{N}(z_t; \sqrt{\bar{\alpha}_t}, (1 - \bar{\alpha}_t)\mathbf{I}), \quad (4)$$

The diffusion model $\epsilon_\theta(z_t, t)$ predicts the noise added to z_t at step t , enabling denoising from z_t to z_{t-1} by removing the predicted noise. The model ϵ_θ is trained by minimizing the following loss function [19]:

$$\min_{\theta} \mathcal{L}(\theta) = \mathbb{E}_{z_0, \epsilon \sim \mathcal{N}(0, I), t} \|\epsilon - \epsilon_\theta(z_t, t)\|_2^2, \quad (5)$$

The DDPM [19] reverse process is a Markov chain of stochastic Gaussian transitions requiring a substantial number of time steps T , which results in prolonged inference. To expedite this process while maintaining sample quality, [29] introduced the Denoising Diffusion Implicit Model (DDIM), offering faster inference with fewer diffusion steps and a deterministic reverse process. Therefore, DDIM is utilized as the scheduler in the Stable Diffusion pipeline in our project. The reverse process under DDIM is defined in Eq. (6).

$$z_{t-1} = \sqrt{\bar{\alpha}_{t-1}} \left(\frac{z_t - \sqrt{1 - \bar{\alpha}_t} \epsilon_\theta}{\sqrt{\bar{\alpha}_t}} \right) + \sqrt{1 - \bar{\alpha}_{t-1}} \epsilon_\theta, \quad (6)$$

VENOM generates UAE from the latent noisy input z_T , which may originate from a Gaussian noise $\mathcal{N}(0, 1)$ or a noisy latent derived from a reference image after forward diffusion. Benefiting from DDIM’s deterministic property [29], we can invert the reverse process by Eq. (7) to encode the reference image into a chosen noisy latent z_{t+1} at any step $t \in [0, 1, \dots, T - 1]$, rather than executing forward diffusion from z_0 . Note that ϵ_θ in Eq. (6) and Eq. (7) is a simplified notation for $\epsilon_\theta(z_t, t)$.

$$z_{t+1} = \sqrt{\bar{\alpha}_{t+1}} \left(\frac{z_t - \sqrt{1 - \bar{\alpha}_t} \epsilon_\theta}{\sqrt{\bar{\alpha}_t}} \right) + \sqrt{1 - \bar{\alpha}_{t+1}} \epsilon_\theta, \quad (7)$$

3.2. Adversarial Guidance with Momentum

The adversarial guidance in VENOM is applied to the latent variable z_{t-1} following each denoising step ($z_t \rightarrow z_{t-1}$) when adversarial perturbation is activated; otherwise, z_{t-1} proceeds to the next denoising step without modification, as shown in Figure 2. Unlike most diffusion-based adversarial attack approaches, which iteratively optimize the latent variable z_t or input embeddings [3, 4, 21], we apply a small adversarial perturbation incrementally at each reverse step, as demonstrated in [7]. This approach reduces visual distortion and enhances the image quality of the generated UAEs.

The adversarial guidance at each reverse diffusion step is similar to FGSM [14] but differs in that it uses an

unrestricted gradient without any l_p -norm constraints. Instead of relying solely on the instantaneous gradient at each step, we introduce a momentum-based approach, where a moving average of past gradients stabilizes the adversarial guidance. This technique allows for consistent adversarial directionality without compromising image quality, effectively guiding the generation towards adversarial examples while maintaining visual fidelity. At each reverse diffusion step t , the adversarial guidance $g(t)$ is calculated as follows:

$$g(t) = \nabla_{x_{t-1}} \log p_f(y_a | x_{t-1}) \quad (8)$$

where y_a is the target label that the adversarial example is intended to misclassify, and x_{t-1} represents the one-step denoised version of x_t during the reverse diffusion process. The adversarial guidance is then incorporated into the reverse diffusion process with momentum, as shown in Eq. (9):

$$z_{t-1}^* = z_{t-1} + sv_t : \begin{cases} v_{t_0} = g(t) & t = t_0 \\ \beta v_{t+1} + (1 - \beta)g(t) & t < t_0 \end{cases} \quad (9)$$

Here, v_t represents the momentum-adjusted adversarial guidance, scaled by a factor s . At the initial step t_0 , v_t is initialized as $g(t_0)$. In subsequent steps, it is computed as an exponentially weighted moving average of previous gradients, controlled by the momentum coefficient β . This momentum-based adversarial guidance smooths the perturbations, reducing the risk of image corruption while ensuring the generation remains adversarially effective.

3.3. Adaptive Control Strategy for Injecting the Adversarial Guidance

As illustrated in Figure 2, the adaptive control strategy functions as a switch that governs when to activate or deactivate adversarial guidance. This straightforward switching mechanism effectively adjusts the strength of the adversarial attack in response to the current state of the latent variable z_t . The detailed procedure is outlined in Algorithm 1. The adversarial guidance is toggled according to the following conditions:

1. **ON**: By default.
2. **OFF**: If x_t is successfully transformed in to an adversarial example.
3. **ON**: if adversarial guidance is detected as OFF, but x_t is no longer adversarial after subsequent denoising.
4. **ON**: If the attack fails twice, adversarial guidance is forcefully kept ON in future iterations.

This adaptive yet simple control strategy enables VENOM to generate UAEs with a high ASR while maintaining superior image quality. To the best of our knowledge, VENOM is the first UAE generation method

Algorithm 1 The Algorithm of VENOM

Require: T : diffusion time steps; f : victim model; N : attack iterations; x : (optional) reference image; y_a : (optional) target label; t_{start} : start step for adversarial guidance

```

 $x_T \leftarrow \text{DDIM\_inversion}(x)$  if  $X$  exists else  $\mathcal{N}(0, 1)$ 
 $z_T \leftarrow \text{VAE\_encoder}(x_T)$ 
adv_guidance  $\leftarrow$  True
for  $N \in [1, 2, \dots, N]$  do
  for  $t \in [T, T - 1, \dots, 0]$  do
    if  $N > 2$  then adv_guidance  $\leftarrow$  True
    end if
 $z_{t-1} \leftarrow \text{reverse\_diffusion\_step}(z_t)$ 
    if adv_guidance == False then
       $x_{t-1} \leftarrow \text{VAE\_decoder}(z_{t-1})$ 
      if  $y_a \neq \text{argmax}_f(x_{t-1})$  then
adv_guidance  $\leftarrow$  True
      end if
    end if
    if  $0 < t \leq t_{start}$  and adv_guidance then
       $x_{t-1} \leftarrow \text{VAE\_decoder}(z_{t-1})$ 
      if  $y_a == \text{argmax}_f(x_{t-1})$  then
adv_guidance  $\leftarrow$  False
      end if
      if  $t = t_{start}$  then
 $v \leftarrow \nabla_{x_{t-1}} \log p_f(y_a | x_{t-1})$ 
      end if
 $v \leftarrow \beta v + (1 - \beta) \nabla_{x_{t-1}} \log p_f(y_a | x_{t-1})$ 
 $z_{t-1} \leftarrow z_{t-1} + sv$ 
      end if
    end for
 $x_0 \leftarrow \text{VAE\_decoder}(z_0)$ 
    if  $y_a == \text{argmax}_f(x_0)$  then break
    end if
  end for
return  $x_0$ 

```

that dynamically controls attack strength and achieves the best image quality among existing approaches.

4. Experiments

VENOM is designed to generate both NAEs and UAEs, and in this section, we evaluate its performance in both modes. We present comprehensive comparisons between VENOM and existing diffusion-based adversarial attack methods, focusing on both image quality and attack efficacy. Additionally, we conduct an ablation study to assess the impact of the adaptive control strategy and momentum on the adversarial guidance.

4.1. Experimental Settings

Dataset and models: We evaluate the NAE and UAE modes separately because they require different settings,



Figure 3. Note that most of existing adversarial attack methods can only work on given reference images, thus we generate the same reference NAEs from identical Gaussian noise and use basic class names as text prompts, facilitating a fair comparison across different attack strategies displayed in each column. The top row shows clean images produced by the stable diffusion model without adversarial perturbation, serving as a reference. Corrupted NAEs are outlined with red borders to ensure clear visual distinction.

and some works support only one of them. [3, 21]. **NAE mode:** We generate NAEs from random Gaussian noise using text prompts derived from ImageNet labels. To ensure semantic alignment between generated images and their corresponding labels, we filter out ambiguous labels that are problematic for the Stable Diffusion model (e.g., “drake”, “black widow”). Ambiguity is assessed by verifying whether a pretrained ResNet50 correctly classifies the generated image prompted by the label; labels leading to misclassification are discarded. This filtering process yields a subset of 466 usable labels from the original 1,000 ImageNet labels. (In the absence of adversarial perturbations, 72% of clean images generated with filtered, unambiguous labels are accurately classified by a pretrained ResNet-50 model. However, without label filtering to remove ambiguous cases, the classification accuracy drops significantly to 40%.) We generate five samples per selected class, resulting in a total of 2,330 NAEs. **UAE mode:** VENOM also generates UAEs based on reference images. We evaluate its performance on generating UAEs using the ImageNet-Compatible Dataset.¹ We utilize the Stable Diffusion model [27] and DDIM [29] sampling for generating both NAEs and UAEs. Refer to the supplementary material for more implementation details.

Evaluation metrics: We evaluate the quality of UAEs and NAEs based on image quality and attack efficacy. Image quality is assessed using FID [18], SSIM [35], LPIPS [37], Inception Score (IS) [28], TReS score [13], and CLIP score [17]. Attack efficacy is measured by the attack success rate (ASR) against both white box and black box models and defense methods such as Neural Representation Purifier (NRP) [25], Random Smooth-

ing (RS) [5], adversarial training [22] and DiffPure [26].

4.2. Synthesizing NAEs from Random Noise

To date, three diffusion model-based adversarial attack methods have been proposed to synthesize Natural Adversarial Examples (NAEs) from random noise: SD-NAE [21], AdvDiffuser [4], and AdvDiff [7]. These methods, however, utilize different diffusion models and inputs. Specifically, SD-NAE accepts text prompts and is based on Stable Diffusion [27] with DDIM sampling [29], while AdvDiffuser and AdvDiff take class labels as input and are built upon Guided Diffusion [9] with DDPM sampling and Latent Diffusion [27] with DDIM sampling, respectively. Our proposed method, VENOM, employs text prompts and leverages Stable Diffusion with DDIM sampling.

To ensure a fair comparison under consistent conditions, we re-implement AdvDiff and AdvDiffuser using the same pretrained Stable Diffusion model and DDIM sampling. This standardization allows us to provide all adversarial attack methods with identical inputs and to rigorously evaluate the quality of the generated NAEs. Image quality is assessed using standard image quality evaluation metrics, and attack efficacy is evaluated based on the Attack Success Rate (ASR) against white-box models, black-box models, and various defense methods.

Image quality assessment: Most image quality evaluation metrics—such as FID, SSIM, and LPIPS—require reference images for comparison. Therefore, we generate clean images without adversarial guidance to serve as references. Table 1 reports the metric scores for NAEs generated by different methods, with arrows indicating whether higher or lower values are preferable. Our VENOM method achieves superior scores across FID, SSIM, LPIPS, and CLIP Score, demonstrating en-

¹https://github.com/cleverhans-lab/cleverhans/tree/master/cleverhans_v3.1.0/examples/nips17_adversarial_competition_dataset

hanced image quality that is structurally and perceptually closer to the originals and better aligned with textual descriptions than other methods. To provide qualitative insights beyond quantitative metrics, we display NAEs generated by various approaches in Figure 3. All images are generated from identical random noise inputs to facilitate direct visual comparison. We observe that other methods exhibit instability, introducing artifacts in certain samples: AdvDiff induces strong distortions, SD-NAE produces images with misaligned labels, and AdvDiffuser excessively denoises some examples. This instability suggests that their NAE generation capabilities are inconsistent, with some samples rendered satisfactorily while others are significantly corrupted due to the injection of adversarial guidance.

Table 1. Image quality assessment of NAEs. The best result is bolded.

Method	FID ↓	SSIM ↑	LPIPS ↓	IS ↑	CLIP ↑
SD-NAE [21]	27.78	0.2502	0.5601	42.27	0.8477
AdvDiffuser [4]	21.34	0.7866	0.1608	44.40	0.8765
AdvDiff [7]	34.25	0.8539	0.0763	30.20	0.8691
VENOM (Ours)	14.49	0.8771	0.0583	41.12	0.8789

Attack efficacy: We employ a pretrained ResNet50[15] as the victim model for all attack methods to generate NAEs. We evaluate the efficacy of different attacks by comparing their attack success rates (ASRs) on both white-box and black-box models. The white-box model is ResNet50 (Res50), while the black-box models include Inception-v3 (Inc-v3)[32], Vision Transformer (ViT)[10], and MLP-Mixer Base (Mix-B)[34], representing convolutional neural network (CNN), transformers, and multi-layer perceptrons (MLPs) architectures, respectively. Additionally, we assess the robustness of various defense methods against these attacks, including adversarially trained ResNet50 (Res50-adv)[11], NRP[25], RS[5], and DiffPure[26]. Table 2 summarizes the results of our attack efficacy evaluation. VENOM demonstrates the strongest performance in the white-box setting among all methods tested. However, its transferability to black-box models is markedly poor, as evidenced by the data in Table 2. While SD-NAE appears to achieve superior transferability and robustness against defense methods, a combined analysis of Table 2 and Figure 3 reveals that the reported high ASRs are misleading. Specifically, SD-NAE, AdvDiffuser, and AdvDiff suffer from instability in NAE generation; notably, SD-NAE and AdvDiffuser yield invalid NAEs in nearly half of the cases. A fair evaluation is infeasible without manual filtering of corrupted examples via human inspection, making white-box attack performance the only reliable metric.

Table 2. Attack success rates of NAEs against white-box (1st row), black-box models (2-4 rows), and various defense methods (5-8 rows). The best result is bolded.

Method	SD-NAE	AdvDiff	AdvDiffuser	VENOM (ours)
Res50 [15]	55.15	98.80	31.38	99.18
Inc-V3 [32]	57.33	60.65	41.12	50.39
ViT [10]	50.86	42.45	33.05	34.98
Mix-B [34]	61.51	58.20	45.20	50.80
Res50-adv [11]	53.40	39.02	36.87	34.68
NRP [25]	76.62	85.63	66.61	85.46
RS [5]	55.54	54.42	39.06	44.98
DiffPure [26]	55.24	52.54	38.33	43.70

4.3. Synthesizing UAEs from Reference Images

Attack efficacy: We generate UAEs using existing images from the ImageNet-compatible dataset and evaluate the attack efficacy of different methods using the same metrics as for NAEs. The results are presented in Table 3, and Figure 4 showcases examples of the generated UAEs. A comparison between Figures 4 and 3 reveals that the adversarial examples are visually almost identical to the original clean images across all attack methods, differing only in minor details. This high fidelity ensures the reliability of the attack efficacy evaluation metrics, as all UAEs are valid, contrasting with the potentially misleading results observed in Table 2. In Table 3, “VENOM” denotes the targeted attack version of our method, while “VENOM-*u*” represents the untargeted variant. We include VENOM-*u* for a fair comparison with DiffAttack [3], which operates in an untargeted manner. The untargeted attack is implemented by setting the target label y_a to the ground truth label y and reversing the gradient sign in Eq. (8).

The untargeted version exhibits strong attack potency against all defense methods. DiffAttack demonstrates superior transferability on transformer and MLP based models but lower ASRs against the defense methods. Conversely, AdvDiff achieves the best performance in white-box attack but shows the poorest results in transferability and effectiveness against defense methods. We also evaluated the untargeted version of AdvDiff, which reportedly has good transferability; however, the image quality was significantly degraded, leading us to deem them invalid UAEs. Overall, our VENOM method exhibits a well-balanced performance across these evaluations, despite not being specifically designed for generating UAEs based on reference images.

Image quality assessment: Figure 4 illustrates that UAEs generated by different methods exhibit relatively high imperceptibility. Table 4 presents the scores from various image quality assessment metrics. Notably, the highest scores across different metrics are distributed among different attack methods, indicating that image quality evaluations vary depending on the assessment

Table 3. Attack success rates of UAEs against white-box (1st row), black-box models (2-4 rows), and various defense strategies (5-8 rows). The best result is bolded.

Method	DiffAttack	AdvDiff	VENOM	VENOM- <i>u</i>
Res50 [15]	94.30	99.80	98.70	98.70
Inc-V3 [32]	70.80	36.52	45.80	71.00
Vit [10]	50.40	12.83	17.20	40.60
Mix-B [34]	61.10	29.24	36.00	59.40
Res50-adv [11]	47.00	33.13	37.90	53.30
NRP [25]	85.91	77.34	78.40	90.10
RS [5]	65.60	31.39	42.20	67.90
DiffPure [26]	56.30	25.44	34.60	60.10

standards. The untargeted variant VENOM-*u* attains slightly lower scores compared to DiffAttack, which can be attributed to its deviation from the real image distribution due to untargeted adversarial guidance. Nevertheless, the targeted version VENOM demonstrates strong overall performance (achieving the best or second-best scores across all metrics) by effectively balancing high perceptual similarity (LPIPS), structural consistency (SSIM), and superior image quality and diversity (TReS, FID and IS).

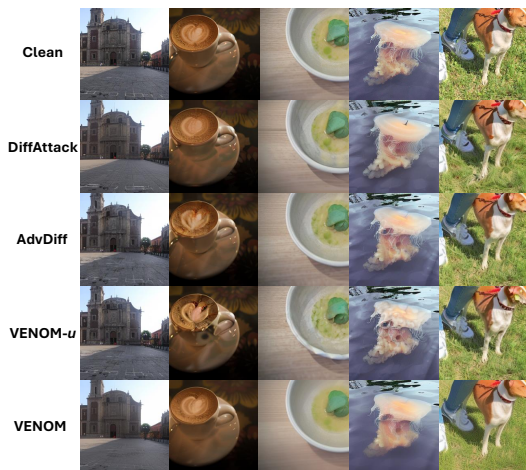


Figure 4. UAEs generated with different attack methods from reference clean images. Please zoom in to compare details.

Table 4. Image quality assessment of UAEs, the best result is bolded, and the second best is marked underlined.

Method	FID ↓	SSIM ↑	LPIPS ↓	IS ↑	TReS ↑
DiffAttack [3]	55.84	0.7166	0.1404	30.11	63.83
AdvDiff [7]	34.52	0.2273	0.7123	42.60	60.63
VENOM- <i>u</i>	62.15	0.6788	0.1856	22.72	61.04
VENOM	<u>36.40</u>	<u>0.7151</u>	0.1399	<u>36.80</u>	66.26

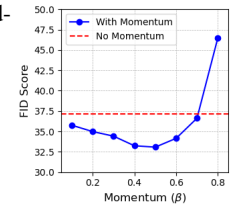
4.4. Ablation Study

Table 5 presents the effects of the momentum (Mo) and adaptive control strategy (AS) modules in VENOM. The

Table 5. Ablation study evaluating the impact of the momentum (Mo) and adaptive control strategy (AS) modules.

Mo	AS	FID ↓	Res50	DiffPure
✗	✗	36.11	98.80	50.74
✓	✗	32.50	99.83	49.28
✗	✓	15.09	98.89	43.70
✓	✓	14.49	99.18	45.63

Figure 5. $\beta \sim$ FID



adaptive control strategy primarily enhances image quality, as evidenced by improved FID scores; however, it reduces the ASR against white-box models and defensive mechanism. In contrast, the Momentum module contributes to image quality while compensating for the ASR loss introduced by the AS module. Together, Mo and AS modules achieve an optimal balance between image quality and attack effectiveness within the VENOM framework.

To determine the optimal hyperparameter β for the Momentum module, we illustrate β versus FID scores in Figure 5, which shows that setting $\beta = 0.5$ yields the lowest FID score. The red dashed line in Figure 5 indicates the FID score of images generated without the Momentum module. Thus, we set $\beta = 0.5$ to maintain optimal image quality in the VENOM framework.

4.5. Discussion & Limitation

The UAEs and NAEs generated by VENOM achieve high white-box ASRs; however, their transferability to black-box models is lower compared to [3], which focuses solely on generating UAEs from reference images. We argue that, **the high transferability from other attack methods is attributed to invalid NAEs** that the original image contents are completely distorted (see more in Supplementary Materials). Fairly measuring ASRs across black-box models and image content high-fidelity without extensive human intervention remains challenging.

5. Conclusion

In conclusion, we present VENOM, a novel framework for generating high-quality, text-driven UAEs with enhanced stability and attack efficacy. By incorporating adaptive control and momentum-enhanced gradients, VENOM effectively balances adversarial robustness and image realism while mitigating corruption. Unlike prior methods, it achieves stable perturbations, enabling consistent generation of both NAEs and UAEs from random noise or reference images. Experimental results highlight VENOM’s strong attack success rates and high image fidelity, solidifying its value as a robust tool for advancing adversarial research and enhancing deep learning security.

References

- [1] Tom B. Brown, Nicholas Carlini, Chiyuan Zhang, Catherine Olsson, Paul F. Christiano, and Ian J. Goodfellow. Unrestricted adversarial examples. *CoRR*, abs/1809.08352, 2018. 3
- [2] Nicholas Carlini and David A. Wagner. Towards evaluating the robustness of neural networks. *2017 IEEE Symposium on Security and Privacy (SP)*, pages 39–57, 2016. 1, 3
- [3] Jianqi Chen, Hao Chen, Keyan Chen, Yilan Zhang, Zhengxia Zou, and Zhenwei Shi. Diffusion models for imperceptible and transferable adversarial attack. *IEEE Transactions on Pattern Analysis and Machine Intelligence (TPAMI)*, pages 1–17, 2024. 2, 3, 4, 6, 7, 8
- [4] Xinquan Chen, Xitong Gao, Juanjuan Zhao, Kejiang Ye, and Cheng-Zhong Xu. Advdiffuser: Natural adversarial example synthesis with diffusion models. In *Proceedings of the IEEE/CVF International Conference on Computer Vision (ICCV)*, pages 4562–4572, 2023. 2, 3, 4, 6, 7
- [5] Jeremy Cohen, Elan Rosenfeld, and Zico Kolter. Certified adversarial robustness via randomized smoothing. In *Proceedings of the 36th International Conference on Machine Learning (ICML)*, pages 1310–1320. PMLR, 2019. 6, 7, 8
- [6] Francesco Croce and Matthias Hein. Reliable evaluation of adversarial robustness with an ensemble of diverse parameter-free attacks. In *Proceedings of the 37th International Conference on Machine Learning (ICML)*. JMLR.org, 2020. 1, 3
- [7] Xuelong Dai, Kaisheng Liang, and Bin Xiao. Advdiff: Generating unrestricted adversarial examples using diffusion models. In *The 18th European Conference on Computer Vision (ECCV)*, pages 93–109, Cham, 2025. Springer Nature Switzerland. 2, 3, 4, 6, 7, 8
- [8] Jia Deng, Wei Dong, Richard Socher, Li-Jia Li, Kai Li, and Li Fei-Fei. Imagenet: A large-scale hierarchical image database. In *2009 IEEE Conference on Computer Vision and Pattern Recognition (CVPR)*, pages 248–255, 2009. 3
- [9] Prafulla Dhariwal and Alex Nichol. Diffusion models beat gans on image synthesis. In *Proceedings of the 35th International Conference on Neural Information Processing Systems (NeurIPS)*, Red Hook, NY, USA, 2024. Curran Associates Inc. 6
- [10] Alexey Dosovitskiy, Lucas Beyer, Alexander Kolesnikov, Dirk Weissenborn, Xiaohua Zhai, Thomas Unterthiner, Mostafa Dehghani, Matthias Minderer, Georg Heigold, Sylvain Gelly, Jakob Uszkoreit, and Neil Houlsby. An image is worth 16x16 words: Transformers for image recognition at scale. In *International Conference on Learning Representations (ICLR)*, 2021. 7, 8
- [11] Logan Engstrom, Andrew Ilyas, Shibani Santurkar, and Dimitris Tsipras. Robustness (python library), 2019. 7, 8
- [12] Robert Geirhos, Patricia Rubisch, Claudio Michaelis, Matthias Bethge, Felix A. Wichmann, and Wieland Brendel. Imagenet-trained CNNs are biased towards texture; increasing shape bias improves accuracy and robustness. In *International Conference on Learning Representations (ICLR)*, 2019. 3
- [13] S Alireza Golestaneh, Saba Dadsetan, and Kris M Kitani. No-reference image quality assessment via transformers, relative ranking, and self-consistency. In *Proceedings of the IEEE/CVF Winter Conference on Applications of Computer Vision (WACV)*, pages 3209–3218, 2022. 6
- [14] Ian J. Goodfellow, Jonathon Shlens, and Christian Szegedy. Explaining and harnessing adversarial examples. In *3rd International Conference on Learning Representations (ICLR), 2015, San Diego, CA, USA, May 7-9, 2015, Conference Track Proceedings*, 2015. 1, 3, 4
- [15] Kaiming He, X. Zhang, Shaoqing Ren, and Jian Sun. Deep residual learning for image recognition. *2016 IEEE Conference on Computer Vision and Pattern Recognition (CVPR)*, pages 770–778, 2015. 7, 8
- [16] Dan Hendrycks, Kevin Zhao, Steven Basart, Jacob Steinhardt, and Dawn Xiaodong Song. Natural adversarial examples. *2021 IEEE/CVF Conference on Computer Vision and Pattern Recognition (CVPR)*, pages 15257–15266, 2019. 3
- [17] Jack Hessel, Ari Holtzman, Maxwell Forbes, Ronan Le Bras, and Yejin Choi. CLIPScore: A reference-free evaluation metric for image captioning. In *Proceedings of the 2021 Conference on Empirical Methods in Natural Language Processing (EMNLP)*, pages 7514–7528, Online and Punta Cana, Dominican Republic, 2021. Association for Computational Linguistics. 6
- [18] Martin Heusel, Hubert Ramsauer, Thomas Unterthiner, Bernhard Nessler, and Sepp Hochreiter. Gans trained by a two time-scale update rule converge to a local nash equilibrium. In *Proceedings of the 31st International Conference on Neural Information Processing Systems (NeurIPS)*, page 6629–6640, Red Hook, NY, USA, 2017. Curran Associates Inc. 6
- [19] Jonathan Ho, Ajay Jain, and Pieter Abbeel. Denoising diffusion probabilistic models. In *Proceedings of the 34th International Conference on Neural Information Processing Systems (NeurIPS)*, Red Hook, NY, USA, 2020. Curran Associates Inc. 3, 4
- [20] Zhan Hu, Siyuan Huang, Xiaopei Zhu, Xiaolin Hu, Fuchun Sun, and Bo Zhang. Adversarial texture for fooling person detectors in the physical world. *2022 IEEE/CVF Conference on Computer Vision and Pattern Recognition (CVPR)*, pages 13297–13306, 2022. 3
- [21] Yueqian Lin, Jingyang Zhang, Yiran Chen, and Hai Li. SD-NAE: Generating natural adversarial examples with stable diffusion. In *The Second Tiny Papers Track at International Conference on Learning Representations (ICLR)*, 2024. 2, 3, 4, 6, 7
- [22] Aleksander Madry, Aleksandar Makelov, Ludwig Schmidt, Dimitris Tsipras, and Adrian Vladu. Towards deep learning models resistant to adversarial attacks. In *International Conference on Learning Representations (ICLR)*, 2018. 1, 3, 6
- [23] Puneet Mangla, Surgan Jandial, Sakshi Varshney, and Vineeth N. Balasubramanian. AdvGAN++: Harnessing la-

- tent layers for adversary generation. *2019 IEEE/CVF International Conference on Computer Vision Workshop (ICCVW)*, pages 2045–2048, 2019. 2, 3
- [24] Claudio Michaelis, Benjamin Mitzkus, Robert Geirhos, Evgenia Rusak, Oliver Bringmann, Alexander S. Ecker, Matthias Bethge, and Wieland Brendel. Benchmarking robustness in object detection: Autonomous driving when winter is coming. *arXiv preprint arXiv:1907.07484*, 2019. 3
- [25] Muzammal Naseer, Salman Khan, Munawar Hayat, Fahad Shahbaz Khan, and Fatih Porikli. A self-supervised approach for adversarial robustness. In *IEEE/CVF Conference on Computer Vision and Pattern Recognition (CVPR)*, 2020. 6, 7, 8
- [26] Weili Nie, Brandon Guo, Yujia Huang, Chaowei Xiao, Arash Vahdat, and Anima Anandkumar. Diffusion models for adversarial purification. In *International Conference on Machine Learning (ICML)*, 2022. 6, 7, 8
- [27] Robin Rombach, A. Blattmann, Dominik Lorenz, Patrick Esser, and Björn Ommer. High-resolution image synthesis with latent diffusion models. *2022 IEEE/CVF Conference on Computer Vision and Pattern Recognition (CVPR)*, pages 10674–10685, 2021. 2, 3, 6
- [28] Tim Salimans, Ian Goodfellow, Wojciech Zaremba, Vicki Cheung, Alec Radford, and Xi Chen. Improved techniques for training gans. In *Proceedings of the 30th International Conference on Neural Information Processing Systems (NeurIPS)*, page 2234–2242, Red Hook, NY, USA, 2016. Curran Associates Inc. 6
- [29] Jiaming Song, Chenlin Meng, and Stefano Ermon. Denoising diffusion implicit models. In *International Conference on Learning Representations (ICLR)*, 2021. 4, 6
- [30] Yang Song, Rui Shu, Nate Kushman, and Stefano Ermon. Constructing unrestricted adversarial examples with generative models. In *Proceedings of the 32nd International Conference on Neural Information Processing Systems (NeurIPS)*, page 8322–8333, Red Hook, NY, USA, 2018. Curran Associates Inc. 2, 3
- [31] Christian Szegedy, Wojciech Zaremba, Ilya Sutskever, Joan Bruna, Dumitru Erhan, Ian J. Goodfellow, and Rob Fergus. Intriguing properties of neural networks. In *2nd International Conference on Learning Representations (ICLR)*, 2014. 1, 3
- [32] Christian Szegedy, Vincent Vanhoucke, Sergey Ioffe, Jonathon Shlens, and Zbigniew Wojna. Rethinking the inception architecture for computer vision. *2016 IEEE Conference on Computer Vision and Pattern Recognition (CVPR)*, pages 2818–2826, 2015. 7, 8
- [33] Rohan Taori, Achal Dave, Vaishaal Shankar, Nicholas Carlini, Benjamin Recht, and Ludwig Schmidt. Measuring robustness to natural distribution shifts in image classification. In *Proceedings of the 34th International Conference on Neural Information Processing Systems (NeurIPS)*, Red Hook, NY, USA, 2020. Curran Associates Inc. 3
- [34] Ilya Tolstikhin, Neil Houlsby, Alexander Kolesnikov, Lucas Beyer, Xiaohua Zhai, Thomas Unterthiner, Jessica Yung, Andreas Steiner, Daniel Keysers, Jakob Uszkoreit, Mario Lucic, and Alexey Dosovitskiy. Mlp-mixer: an all-mlp architecture for vision. In *Proceedings of the 35th International Conference on Neural Information Processing Systems (NeurIPS)*, Red Hook, NY, USA, 2024. Curran Associates Inc. 7, 8
- [35] Zhou Wang, A.C. Bovik, H.R. Sheikh, and E.P. Simoncelli. Image quality assessment: from error visibility to structural similarity. *IEEE Transactions on Image Processing (TIP)*, 13(4):600–612, 2004. 6
- [36] Chaowei Xiao, Bo Li, Jun-Yan Zhu, Warren He, Mingyan Liu, and Dawn Song. Generating adversarial examples with adversarial networks. In *Proceedings of the 27th International Joint Conference on Artificial Intelligence (IJCAI)*, page 3905–3911. AAAI Press, 2018. 2, 3
- [37] Richard Zhang, Phillip Isola, Alexei A. Efros, Eli Shechtman, and Oliver Wang. The unreasonable effectiveness of deep features as a perceptual metric. *2018 IEEE/CVF Conference on Computer Vision and Pattern Recognition (CVPR)*, pages 586–595, 2018. 6
- [38] Zhengli Zhao, Dheeru Dua, and Sameer Singh. Generating natural adversarial examples. In *International Conference on Learning Representations (ICLR)*, 2018. 3